



Dynamics of spreading of liquid on a hydrogel substrate

Tadashi Kajiya, Adrian Daerr, Laurent Royon, Tetsuharu Narita, François Lequeux, Laurent Limat

► To cite this version:

Tadashi Kajiya, Adrian Daerr, Laurent Royon, Tetsuharu Narita, François Lequeux, et al.. Dynamics of spreading of liquid on a hydrogel substrate. European Coating Symposium, ECS 2011, Martti Toyvakka; Parvez Alam; Jarkko J. Saarinen; Mari Nurmi; Jani Kniivila; Pauliina Saloranta, Jun 2011, Turku, Finland. pp.272. hal-02379861

HAL Id: hal-02379861

<https://hal.archives-ouvertes.fr/hal-02379861>

Submitted on 25 Nov 2019

HAL is a multi-disciplinary open access archive for the deposit and dissemination of scientific research documents, whether they are published or not. The documents may come from teaching and research institutions in France or abroad, or from public or private research centers.

L'archive ouverte pluridisciplinaire **HAL**, est destinée au dépôt et à la diffusion de documents scientifiques de niveau recherche, publiés ou non, émanant des établissements d'enseignement et de recherche français ou étrangers, des laboratoires publics ou privés.

Dynamics of spreading of liquid on a hydrogel substrate

Tadashi Kajiya¹, Adrian Daerr¹, Laurent Royon¹, Tetsuharu Narita²,
François Lequeux² and Laurent Limat¹

¹Laboratoire MSC, UMR 7057 CNRS, Université Paris Diderot, 10 rue Alice Domon et Léonie Duquet, 75205 Paris Cedex 13, France

²PPMD-SIMM, UMR 7615, CNRS, UPMC, ESPCI ParisTech, 10 rue vauquelin, 75231 Paris Cedex 05, France

Corresponding author: tadashi.kajiya@univ-paris-diderot.fr

Keywords: wetting, spreading, moving contact line, gel

1. Introduction

Gels are materials which have been attracting continued interest as they are intriguing state of matter in physical and chemical sciences [1] and they also have promising technological potentials in many application fields. The understanding and control of interfacial properties of gels is of crucial importance in several promising applications: they determine adhesion and friction [2] (e.g. cartilage replacement), surface tension and wetting properties (e.g. soft coatings), optical properties (e.g. anticondensation coatings), effects on bacterial motility [3]. Of those problems about the interfacial properties of gels, here we are focusing on the problem of wetting.

Compared to general solid materials on which wetting problems have been extensively studied, gels have two specific features which can affect the dynamics of the contact line, i.e., gels are very soft and swells drastically with liquid. Although the effect of the softness (i.e. deformability) and of liquid diffusivity on the dynamics of contact line in wetting processes were studied individually [4-7], the dynamics of the contact line on gel surfaces would be yet different from those cases because these two features exist simultaneously. Several studies have been conducted to characterize the wetting properties on gel surfaces [8, 9], but these studies did not make it clear how the dynamics of contact line is different when it is coupled with the local deformation of the substrate and the diffusion of the liquid.

In this article, we study the wetting and diffusing processes of water droplets on hydrogel substrates. For the precise analysis of the dynamics of the contact line with the existence of the deformation of the substrate and diffusion of the liquid, it is required to measure both the profiles of the droplet and of the substrate simultaneously. By using a grid projection method, we have established a new experimental method for measuring these two profiles simultaneously and dynamically.

2. Experimental Section

For the hydrogel substrate, two gels were prepared: nonionic Poly (vinyl alcohol) (PVA) gels and anionic Poly (2-acrylamido-2-methyl-propane-sulfonic acid -co- acrylamide) (PAMPS-PAAM) gels. Distilled water (Milli-Q Integral; Millipore, USA) was used for liquid droplets.

The processes for the preparation of gel substrates are as follows. The PVA gels were prepared through the cross-linking reaction of poly vinyl alcohol (PVA; Mw = 100,000; Sigma-Aldrich, USA) solution with a cross-linking agent Glutaraldehyde (GA; Sigma-Aldrich, USA) at an acidic condition (pH \approx 2, adjusted by hydrochloric acid). The total mass concentration of polymer was set at 5% and the molar concentration of GA was set at 1 mol%. The PAMPS-PAAM gels were prepared through the radical polymerization of a solution of 2-acrylamido-2-methyl-propane-sulfonic acid (AMPS; Sigma-Aldrich, USA) and acrylamide (AAM; Alfa Aesar, USA) in water with a cross-linking agent, N,N'-methylenebisacrylamide (MBA; Sigma-Aldrich, USA), and with initiators, Potassium persulfate (PS; Sigma-Aldrich, USA) and N,N,N',N'-Tetramethylenediamine (TEMED; Sigma-Aldrich, USA). The molar ratio of monomers was AMPS : AAM = 3 : 7. The total mass concentration of monomer was set at 10 %, and the molar concentrations of MBA, PS, and TEMED were set at 5 mol%, 1 mol%, and 1 mol%, respectively. To obtain a sheet-shaped gel substrate, the gels was prepared between two parallel glass plates which were separated by a silicon rubber spacer with a thickness of 4.5 mm.

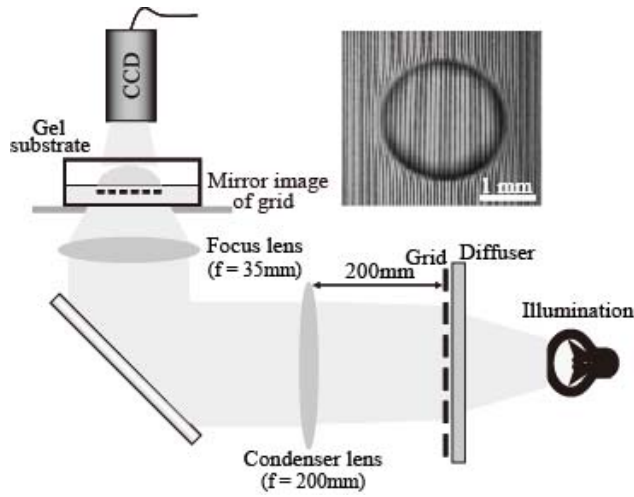


Fig.1 Schematic of the setup for the profile measurement. Using two lenses (converting lens $f=200$ mm, focus lens $f=35$ mm), the mirror image of the grid is projected inside the gel just below the droplet. The image of the grid lines is also shown. Due to the deformation of the interface (air-water and air-gel), the grid lines are distorted.

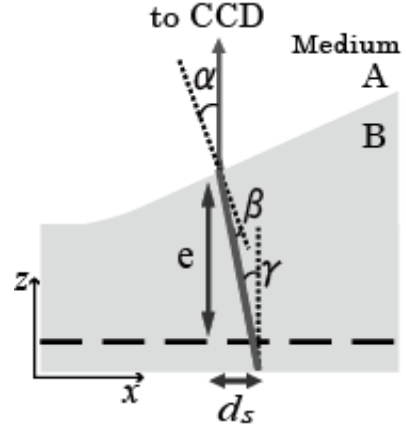


Fig.2 Geometry of the light path that passes through the grid image and is detected by the CCD. As the interface between two mediums A (air) and B (water or gel) of different optical indexes is inclined relative to the horizontal axis x , the light is refracted at the interface. By tracing the light path in each grid line, the original profile can be reconstructed

Figure 1 shows the setup for the profile measurement. The gel substrate was placed on a hollow stage, and a droplet was placed on the substrate with a micropipet. The initial volume of the droplet was fixed to $1 \mu\text{l}$. To measure both the profiles of the droplet and of gel simultaneously, the grid projection method was used [10]. In the grid projection method, the profiles are measured by tracing the distortion of grid lines between before and after the placement of the droplet. The original grid plate was located far from the observation system. The illumination light emitted from the photodiode passed through the grid plate and was converted to a parallel light by an optical lens ($f = 200$ mm). Then the light was guided to the bottom of the substrate, and passed through a focus lens (TV lens $f = 35$ mm: Pentax, Japan). This focus lens projects the mirror image of the grid inside the gel substrate, which is set just below the droplet. With the use of the mirror image, the resolution of the grid lines increases up to 6 times of the original grid lines. The grid image was measured by a CCD camera (A101FC; Basler AG, Germany) which was located above the droplet. The example of the grid image obtained after the placement of droplet is also shown in fig. 1.

The original profile can be reconstructed by tracing the light path which passes through each grid line. As is shown in fig. 2, the shift of the grid line d_s is related to the local slope of the interface $\tan \alpha(x, t)$ between the mediums of different refractive ratios (medium A: air, medium B: water or gel). With geometrical optics, the relation between the shift and slope is given by the following three equations:

$$\sin \alpha = n \sin \beta, \quad (1)$$

$$\gamma = \alpha - \beta, \quad (2)$$

$$\tan \gamma = \frac{d_s}{e}, \quad (3)$$

where α and β are the angles of the light path in mediums A and B with respect to the normal to the interface, γ is the angle of the light path in medium B with respect to the vertical axis, n is the refractive index of medium B (since the water volume fraction in the gel is considerably large, we used the value of water $n = 1.33$ in the whole range of experiment). By solving eqs. (1) - (3) numerically, the local slope of the interface $\tan \alpha$ was obtained from d_s , and the whole profile was obtained by integrating $\tan \alpha$ in a horizontal direction x .

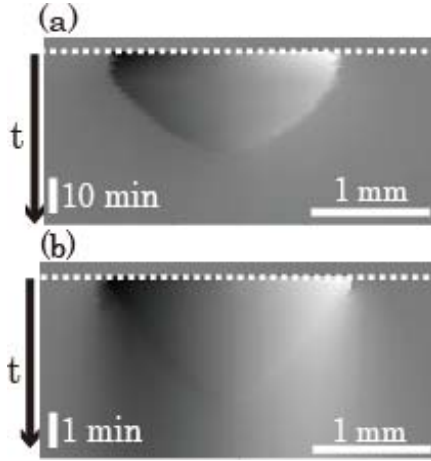


Fig.3 Spatio-temporal diagram of the shift distance of each grid line. The shift distance d_s is proportional to the gray-scale: the dark region means that the grid shifts to left and the bright region indicates the grid shifts to right. (a) PVA gel. (b) PAMPS-PAAM gel.

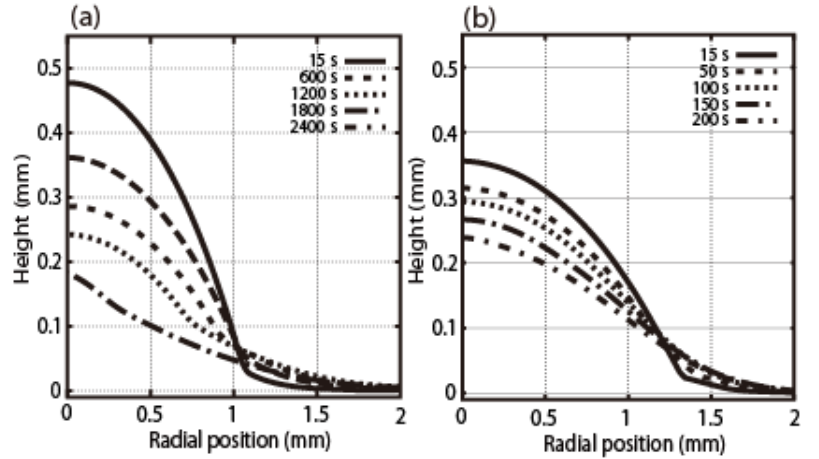


Fig.4 Half cross sections of the reconstructed profiles of the droplet and of substrate for 5 different time steps. (a) PVA gel. (b) PAMPS-PAAM gel. On both gels, the local deformation of the gel grows in the vicinity of the contact line.

3. Results and Discussion

Figure 3 shows the spatio-temporal diagram of the shift distance of the grid lines d_s in one cross section of the droplet. Figure 3 (a) is the results on PVA gel, and (b) is on PAMPS gel. It is seen that after the droplet is placed on a substrate, the grid lines in the regions of the droplet shift from their initial positions to certain distances. In the left side of the center of the droplet, the lines shift to left, while the lines shift to right in the right side.

Just after the droplet is placed on a substrate, there exist a large discontinuity of d_s between the region where the droplet was placed and the other region, i.e., d_s varies sharply at the edge of the droplet. As the water diffuses from the droplet to the gel d_s becomes smaller in the droplet region. On the other hand, the region where d_s has a non-zero value extends from the initial position of the contact line.

Using the procedure mentioned in the previous section, the original profiles and their time evolution can be reconstructed from the data in fig. 3. Figure 4 shows the half cross sections of the profiles (the height against the radial position) of the droplet and gel substrate for 5 different time steps. It is seen that during the diffusion process of the droplet into the gel substrate, both the profiles of the droplet and substrate vary. At the initial stage ($t = 15$ s), the contact line of the droplet is seen clearly, i.e., there exists a discontinuity of the slope between the region of the droplet and substrate. As the water diffuses from the droplet into the substrate, the height of the droplet region decreases, while the height of the substrate in the vicinity of the contact line increases. At a late stage (1200 s for PVA and 100 s for PAMPS-PAAM), the horizontal scale of the deformation reaches the order of 1 mm, which is considerably larger than the typical deformation extent that was observed in the wetting problem on elastomers [11]. From this feature, we consider that the deformation of the gel substrate is mainly caused by the swelling effect with solvent, and not by the balance between the elastic force and vertical component of surface tension.

As the water diffusion proceeds, the boundary between the droplet and substrate becomes less clear and it is difficult to observe the position of the contact line directly (especially on the PAMPS gel substrate). Even in that stage, it is still possible to detect the contact line by using the curvature in the central region. Due to the effect of the surface tension, the droplet region takes a profile of a spherical cap having a uniform curvature. Therefore, the position of the contact line can be detected as the point where the actual profile deviates from the extrapolation of the curvature at the center.

Figure 5 shows the behavior of the contact line of the droplet on a PAMPS-PAAM gel substrate. Here, the radius of the droplet against the time is plotted in fig. 5 (a), and the angles of the droplet and substrate (with respect to the horizontal plane) against the time are plotted in fig. 5 (b).

In fig. 5 (a), it is seen that the contact line undergoes two different states. Just after the droplet is placed on the substrate, the contact line is pinned, i.e., it does not move during a certain period. Then the contact line starts to recede and it continues to recede until the end of the diffusion.

By comparing fig. 5 (a) with (b), it is clearly seen that the motion of the contact line is strongly coupled with the time variation of the angles. At the first stage when the contact line is pinned, there exists a large difference between θ_{drop} and θ_{gel} . As the water diffusion proceeds, θ_{drop} and θ_{gel} come close to each other, and it is only at the moment where these two angles almost corresponds that the contact line starts to recede. This result means that when a contact line recedes on a PAMPS-PAAM gel substrate, apparently it has a finite receding contact angle, but the actual receding contact angle with respect to the inclined substrate $\theta_{drop} - \theta_{gel}$ is almost 0° .

4. Conclusion

A new experimental technique based on a grid projection method is used for studying dynamics of spreading of liquid on a hydrogel substrate. Our results show that the dynamics of the contact line on hydrogel substrates are quite different from those observed for general solid materials, especially for the coupling between the pinning-receding motions of the contact line and the angles of the droplet and substrate. To understand the receding process of the contact line, the important factor is that the diffusion of the liquid can change the wetting property of the gel surface dynamically. For the detailed analysis of the present phenomena, solving the combined equations of water diffusion into gel and the balance of interfacial tensions at the contact line is required, which will be conducted as our future works.

References

1. M. Doi, *J. Phys. Soc. Jpn.* **78**, 052001 (2009).
2. J. P. Gong, T. Kurokawa, T. Narita, G. Kagata, Y. Osada, G. Nishimura, and M. Kinjo *J. Am. Chem. Soc.* **123**, 5582-5583 (2001).
3. D. Julkowska, M. Obuchowski, I. B. Holland, and S. J. S  ror, *Microbiology* **150**, 1839-1849 (2004).
4. M. E. R. Shanahan and P. G. de Gennes, *R. Acad. Sci. Paris* **302**, Ser. II, 517 (1986).
5. A. Carr  , J. C. Gastel, and M.E.R. Shanahan, *Nature* **379**, 432-434 (1996).
6. C. W. Extrand and Y. Kumagai, *J. Coll. Int. Sci.* **184**, 191-200 (1996).
7. L. Bacri and F. B. Wyart, *Eur. Phys. J. E* **3**, 87-97 (2000).
8. D. Kaneko, J. P. Gong, M. Zr  nyi, and Y. Osada, *J. Pol. Sci. B* **72**, 562-572 (2005).
9. M. Banaha, A. Daerr, and L. Limat, *Eur. Phys. J. Special Topics* **166**, 185-188 (2009).
10. M. Torralba, J. R. Castrejon-Pita, A. A. Castrejon-Pita, G. Huelsz, J. A. del Rio, and J. Ortin, *Phys. Rev. E* **72**, 016308 (2005).
11. R. P. Camara, G. K. Auernhammer, K. Koynov, S. Lorenzoni, R. Raiteri, and E. Bonaccorso, *Soft Matter* **5**, 3611-3617 (2009).

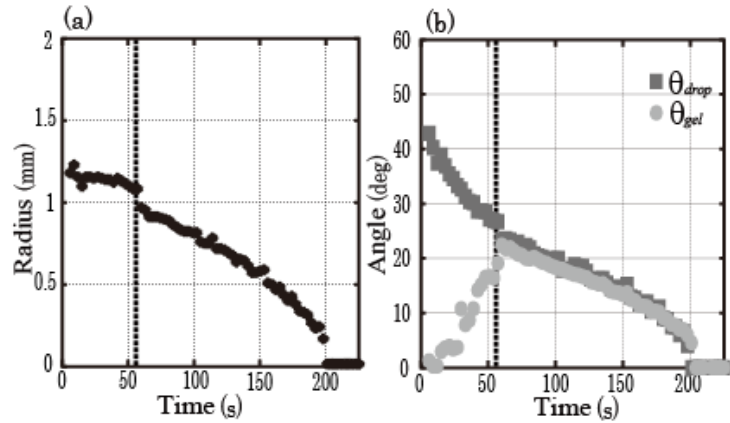


Fig.5 Plot of the (a) radius of the droplet and (b) angles of the droplet and gel substrate against the time on a PAMPS-PAAM gel substrate.